The Role of Parameter Variations in the Static and Dynamic Characteristics of Quantum Dot Lasers by Using Circuit-Level Modeling

M. Razm-Pa, and F. Emami, *Member, IAENG*

***Abstract*—Quantum dot semiconductor lasers are studied by using an equivalent circuit model. There are many circuit models in literature and we simulated the static and dynamic responses of these circuit models by utilizing HSPICE circuit simulator. In this work, the rate equations are applied to the laser behaviors and it is found that for a self-assembled InGaAs-GaAs quantum dot Laser, the laser coverage factor increment can increases the laser threshold current, the external quantum efficiency, the output power and the modulation bandwidth. It is shown that, for lowered inhomogeneous broadening factor there is more optical gain in these lasers.**

***Index Terms*—Quantum dot lasers, equivalent circuit modeling, rate equations, modulation response**

I. Introduction

SEMICONDUCTOR quantum dot (QD) lasers are presented to show a much higher performance compared to usual quantum-well (QW) lasers, in many aspects including threshold current, thermal stability, modulation bandwidth, and spectral band-width, that is similar to an impulse function due to discrete mode density [1]. QD lasers have better carrier confinement with respect to the QW lasers due to three-dimensional confinement which make them as ideal candidates for especial applications such as quantum information. After the appearance of self-assembled (SA) InAs/GaAs QD lasers with a lasing wavelength higher than 1.3μm, detailed study was carried out on their predicted function that will happen in photonic networks. These nanoscale devices are used to solve the well-known problem of "power-speed-tradeoff" too. During the last decade, other applications of SAQDs in ultra-fast semiconductor optical amplifiers, QD-based Mach-Zehnder interferometer and vertical cavity QD switches are reported.

The most useful and well-known method to study the dynamics of the carrier and photon in lasers is to solve rate equations for carriers and photons. Recently, some circuit models are introduced for QD, QW, and bulk lasers modeling [2]–[7].

Manuscript received Dec. 8, 2011. This work was supported in part by the Optoelectronic Research Center, Electronic Department of Shiraz University of Technology.

M. Razm-Pa is with the Islamic Azad University, Boushehr Branch, Boushehr, Iran (e-mail: mahdirazmpa@yahoo.com).

F. Emami was with the Optoelectronic Research Center, Electronic Department of Shiraz University of Technology, Shiraz, Iran (corresponding author: phone: 0098-711-7266-262; fax: 0098-711-7353-502; e-mail: emami@sutech.ac.ir).

In this paper, we have studied the effect of coverage and inhomogeneous factors on L-I curve and the modulation response of SA InAs/GaAs QD lasers, based on the developed models. The results obtained in this study are matched with the numerical results reported by other researchers [8]-[10].

The article is organized as follows:

Section II explains the physics and theory of SA InAs/GaAs QD lasers. Section III describes the rate equations for QD lasers and introduces an equivalent circuit models for rate equations, and the simulation results are provided in section IV. Finally, the conclusions are presented in section V.

II. Theory of SA QD Semiconductor Lasers

Using the SA processes for fabricating a QD laser, it is possible to have wide variety of different semiconductor lasers. Depend on the discrete energy levels of a QD laser, one important aspect of SAQD lasers is the carrier relaxation (phonon bottleneck problem). Besides of this problem, other physical specifications of SAQDs such as inhomogenous broadening of the optical gain of single dots have important effects. Considering these points, we can use a schematic diagram for energy band of a SAQD laser as shown in Fig. 1 [8].

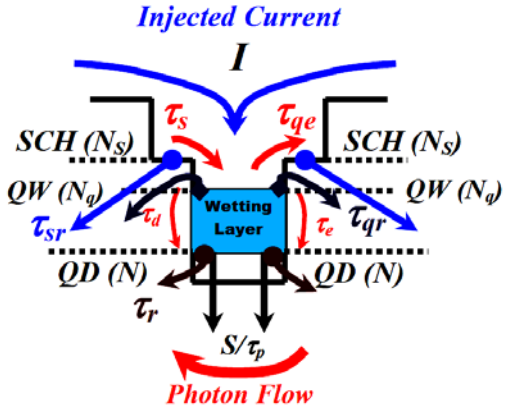

Fig. 1. The active region energy band diagram of a SAQD laser

The injected carriers penetrate across the separate confinement hetero-structure (SCH) layers, relax at the quantum well, and then relax inside the dots. Some carriers are recombined outside (in the quantum well area) and inside the dots in two radiative or non-radiative ways. Above lasing threshold, the ground state carriers emit the photons at lasing mode. It is due to the stimulated emission process. Inside the quantum dot, charge neutrality exists and

ISBN: 978-988-19251-9-0
ISSN: 2078-0958 (Print); ISSN: 2078-0966 (Online)

we assumed that just one electron and one hole are formed. There are some relaxation times which can be expressed as:

τ_s: The diffusion time constant in the SCH region,

τ_{sr}: The carrier recombination in the SCH region,

τ_{qe}: The carrier emission from the QW to the SCH region,

τ_e: The carrier emission from the QD to the QW,

τ_{qr}: The carrier recombination in the QW,

τ_d: The carrier relaxation into the QD, and finally

τ_r: The recombination in the QD.

N_s, N_q and N are the carrier numbers in the separate confinement hetero-structure (SCH) layer, in the QW and QD layers respectively.

The linear optical gain of the active area of QD laser is determined based on density matrix theory, by:

$$g_m^{(1)} = \frac{2.35\sqrt{2\pi}e^2\hbar}{cn_r\varepsilon_0 m_0^2 V_D}\frac{\left|P_{cv}^{\sigma}\right|^2}{\hbar\omega_{cv}}\frac{\xi}{\Gamma_0}(2P-1) \quad (1)$$

Where n_r is the refractive index, $\xi = N_D V_D$ is the coverage factor defined as the product of QDs, N_D, by dot volume V_D, P is the carrier occupation probability, Γ_0 is inhomogeneous broadening. It is considered that the shape of quantum dot to be like a cylinder with the radius of R and the height of H, so we will have $V_D = \pi R^2 H$. If $I_{c,v}$ shows the overlap integral between the envelope functions of an electron and a hole, the transition matrix element will be determined as follows:

$$\left|P_{c,v}^{\sigma}\right|^2 = \left|I_{c,v}\right|^2 M^2 \quad (2)$$

The parameter M^2 is resulted from the first-order **k–p** interaction between the conduction band and valence bands and it is defined as:

$$M^2 = \frac{m_0^*}{12m_e^*}\frac{E_g(E_g+\Delta)}{E_g+\frac{2\Delta}{3}} \quad (3)$$

Where E_g is band gap, m_e^* refers to the effective mass of electron and Δ is spin-orbit interaction energy of the quantum dot material [1] . Based on Pauli Exclusion Principle, carrier occupation probability in the QD ground state is defined as follows:

$$P = \frac{N}{2N_D V_a} \quad (4)$$

In this relation, $V_a = HdlN_W$ is the volume of the active area where d is the strip width, L is the length of cavity and N_W is the dot layers at the active area.

III. Modeling The SA QD Lasers

A. Rate Equations

Carrier behavior in SAQD semiconductor lasers are expressed by a set of coupled differential equations name rate equations. Assume S be the photon number and I the injected current, theses equations are [8], [9]:

$$\frac{dN_s}{dt} = \frac{I}{e} - \frac{N_s}{\tau_s} - \frac{N_s}{\tau_{sr}} + \frac{N_q}{\tau_{qe}}, \quad (5\text{-a})$$

$$\frac{dN_q}{dt} = \frac{N_s}{\tau_s} + \frac{N}{\tau_e} - \frac{N_q}{\tau_{qr}} - \frac{N_q}{\tau_{qe}} - \frac{N_q}{\tau_d} \quad (5\text{-b})$$

$$\frac{dN}{dt} = \frac{N_q}{\tau_d} - \frac{N}{\tau_r} - \frac{N}{\tau_e} - \frac{\left(c/n_r\right)g_m^{(1)}\Gamma}{1+\varepsilon_m\Gamma\, S/V_a}S, \quad (5\text{-c})$$

$$\frac{dS}{dt} = \frac{\left(c/n_r\right)g_m^{(1)}\Gamma}{1+\varepsilon_m\Gamma\, S/V_a}S - \frac{S}{\tau_p} + \frac{\beta N}{\tau_r} \quad (5\text{-d})$$

Where ε_m is the nonlinear gain coefficient and $g_m^{(1)}$ is defined in (1). The photon lifetime in the cavity, τ_p, is achieved by the following relation [9]:

$$\tau_p^{-1} = \left(\frac{c}{n_r}\right)\left[\alpha + \ln\left(\frac{1}{R_1R_2}\right)/2L\right] \quad (6)$$

Where, R_1 and R_2 are the reflectivity of cavity mirror, L is the cavity length, and α is the internal loss of the cavity. As the carrier relaxation is excluded by the filling mode due to Pauli Exclusion Principle, the relaxation rate is expressed as:

$$\tau_d^{-1} = (1-P)\tau_0^{-1} \quad (7)$$

Where, τ_0^{-1} is the relaxation rate when the ground state is not occupied, i.e. $P=0$. If P approaches 1, the relaxation rate is decreased, the result which means a higher level occupation.

Solving the rate equations for the carriers and photons is the most useful method to discuss dynamic and static features of lasers.

B. Equivalent Circuit Model

To analyze the SAQD behavior, an equivalent circuit model was selected and simulated by powerful simulator HSPICE. The carrier population in SCH, WL, and QD is defined using the following relations:

$$N_s = N_{s0}\exp\left(\frac{qV}{n_s kT}\right) \quad (8\text{-a})$$

$$N_q = N_{q0}\exp\left(\frac{qV_q}{n_q kT}\right) \quad (8\text{-b})$$

$$N = N_0\exp\left(\frac{qV_D}{n_D kT}\right) \quad (8\text{-c})$$

Here, N_{s0}, N_{q0} and N_0 are the equilibrium carrier densities at SCH, WL, and QD, respectively, while n_s, n_q and n_D

ISBN: 978-988-19251-9-0
ISSN: 2078-0958 (Print); ISSN: 2078-0966 (Online)

match the ideal diode factors that are considered to be equal to 2 for GaAs-AlGaAs tool [11] , [12] . V_q and V_D are overall voltages for the wetting layer (WL) and QD, respectively. To improve the convergence properties of the model at the simulation time, we change the output power of laser to the new variable of V_m with the following relations [4]:

$$P_{out} = (V_m + \delta)^2 \tag{9}$$

Where δ is an arbitrary constant, which is selected as about 10^{-60} in our simulations. After substituting (8-a)-(8-c) into the (5-a)-(5-c) term by term, and some simplification the following relations can be found:

$$I = \frac{qN_{s0}}{2\tau_s}\left[\exp\left(\frac{qV}{n_s kT}\right)-1+\frac{2\tau_s q}{n_s kT}\exp\left(\frac{qV}{n_s kT}\right)\frac{dV}{dt}\right] + \frac{qN_{s0}}{2\tau_s}\left[\exp\left(\frac{qV}{n_s kT}\right)-1\right]+\frac{qN_{s0}}{\tau_s} \tag{10}$$

With the following definitions:

$$I_{D1} = \frac{qN_{s0}}{2\tau_s}\left[\exp\left(\frac{qV}{n_s kT}\right)-1\right] \tag{11}$$

$$I_{D2} = \frac{qN_{s0}}{2\tau_s}\left[\exp\left(\frac{qV}{n_s kT}\right)-1+\frac{2\tau_s q}{n_s kT}\exp\left(\frac{qV}{n_s kT}\right)\frac{dV}{dt}\right] \tag{12}$$

$$I_{C1} = I_{C2} = \frac{qN_{s0}}{2\tau_s} \tag{13}$$

$$I = I_{D1} + I_{C1} + I_{D2} + I_{C2} \tag{14}$$

And:

$$4I_{T1} = \frac{qN_{q0}}{\tau_{qr}}\left[\exp\left(\frac{qV_q}{n_q kT}\right)-1+\frac{2\tau_{qr}q}{n_q kT}\exp\left(\frac{qV_q}{n_q kT}\right)\frac{dV_q}{dt}\right] + \frac{qN_{q0}}{\tau_{qr}}\left[\exp\left(\frac{qV_q}{n_q kT}\right)-1\right]+2\frac{qN_{q0}}{\tau_{qr}}+ 2q\zeta\ (N)\left[N_{q0}\exp\left(\frac{qV_q}{n_q kT}\right)\right] \tag{15}$$

With the following definitions:

$$I_{D3} = \frac{qN_{q0}}{\tau_{qr}}\left[\exp\left(\frac{qV_q}{n_q kT}\right)-1\right] \tag{16}$$

$$I_{D4} = \frac{qN_{q0}}{\tau_{qr}}\left[\exp\left(\frac{qV_q}{n_q kT}\right)-1+\frac{2\tau_{qr}q}{n_q kT}\exp\left(\frac{qV_q}{n_q kT}\right)\frac{dV_q}{dt}\right] \tag{17}$$

$$I_{C3} = I_{C4} = \frac{qN_{q0}}{\tau_{qr}} \tag{18}$$

$$G_1 = 2q\zeta\ (N)\,\Theta_1 I_{T3} \tag{19}$$

$$\zeta\ (N) = \frac{2N_D V_a - N}{2\tau_0 N_D V_a} \tag{20}$$

$$I_{T3} = I_{D3} + I_{C3} \tag{21}$$

$$4I_{T1} = I_{D3} + I_{D4} + I_{C3} + I_{C4} + G_1 \tag{22}$$

And:

$$\frac{qN_0}{2\tau_r}\left[\exp\left(\frac{qV_D}{n_D kT}\right)-1+\frac{2\tau_r q}{n_D kT}\exp\left(\frac{qV_D}{n_D kT}\right)\frac{dV_D}{dt}\right]+\frac{qN_0}{\tau_r}+ \frac{qN_0}{2\tau_r}\left[\exp\left(\frac{qV_D}{n_D kT}\right)-1\right]+\frac{q\alpha(N)}{\varphi\left[\chi(V_m+\delta)^2\right]}\chi(V_m+\delta)^2 = q\zeta\ (N)\left[N_{q0}\exp\left(\frac{qV_q}{n_q kT}\right)\right] \tag{23}$$

With the following definitions:

$$\chi = \frac{S}{P_{out}} = \frac{\lambda\tau_p}{\eta_c V_a hc} \tag{24}$$

$$I_{D5} = \frac{qN_0}{2\tau_r}\left[\exp\left(\frac{qV_D}{n_D kT}\right)-1+\frac{2\tau_{qr}q}{n_q kT}\exp\left(\frac{qV_D}{n_D kT}\right)\frac{dV_D}{dt}\right] \tag{25}$$

$$I_{D6} = \frac{qN_0}{2\tau_r}\left[\exp\left(\frac{qV_D}{n_D kT}\right)-1\right] \tag{26}$$

$$I_{C5} = I_{C6} = \frac{qN_0}{2\tau_r} \tag{27}$$

$$\alpha(N) = \frac{2.35\sqrt{2\pi}e^2\hbar}{cn_r\varepsilon_0 m_0^2 V_D}\frac{\left|P_{cv}^{\sigma}\right|^2}{\hbar\omega_{cv}}\frac{\xi}{\Gamma_0}\left(\frac{N}{N_D V_a}-1\right)\frac{c}{n_r}\Gamma \tag{28}$$

$$\phi(S) = 1+\frac{\varepsilon_m\Gamma S}{V_a} \tag{29}$$

$$\Theta_1 = \frac{\tau_{qr}}{q}, \qquad N = \Theta_2 I_{T6}, \qquad \Theta_2 = \frac{2\tau_r}{q} \tag{30}$$

$$N_q = \Theta_1 I_{T3}$$

$$G_2 = \frac{q\alpha(N)}{\phi\left[\chi(V_m+\delta)^2\right]}\chi(V_m+\delta)^2 \tag{31}$$

$$G_3 = q\zeta\ (N)\,\Theta_1 I_{T3} \tag{32}$$

$$I_{T6} = I_{D6} + I_{C6} \tag{33}$$

$$I_{D5} + I_{C5} + I_{D6} + I_{C6} + G_2 = G_3 \tag{34}$$

Where β is the coupling efficiency of the spontaneous emission.

From (5-d) and (24):

$$2\tau_p\frac{dV_m}{dt}+V_m = \tau_p\frac{\alpha(N)}{\phi(S)}(V_m+\delta)-\delta+\frac{\tau_p\beta N}{\chi\tau_r(V_m+\delta)} \tag{35}$$

By defining:

ISBN: 978-988-19251-9-0
ISSN: 2078-0958 (Print); ISSN: 2078-0966 (Online)

$$G_4 = \frac{\tau_p \beta N}{\chi \tau_r (V_m + \delta)} \tag{36}$$

$$G_5 = \frac{\alpha(N)}{\phi(S)} \tau_p (V_m + \delta) - \delta \tag{37}$$

$$C_{ph} = 2\tau_p, \qquad R_{ph} = 1 \tag{38}$$

The following relation will satisfy:

$$C_{ph} \frac{dV_m}{dt} + \frac{V_m}{R_{ph}} = G_4 - \delta + G_5 \tag{39}$$

Where E_{out} is converted to V_m through the output power of P_{out} by the following relation:

$$P_{out} = E_{out} = (V_m + \delta)^2 \tag{40}$$

Based on the above equations, it is possible to construct an equivalent circuit as shown in Fig. 2 [2].

Here, *p* and *n* are the electrical terminals of equivalent SA QD laser and P_{out} is the electrical equivalent voltage in the output terminal. Diodes D_1 and D_2, and the current sources of I_{C1} and I_{C2} model charge storage and carrier trapping for SCH carriers. Diodes of D_{w1} and D_{w2}, current sources of I_{CW1} and I_{CW2} present the charge storage and carrier emission in WL, while G_{r1} are expressed for carrier recombination effects. Current source of $4I_{T1}$ express the carrier trapping by WL. Diodes of D_{D1} and D_{D2}, and current sources of I_{CD1} and I_{CD2} express the charge storage and carrier emission in QD, while G_{s2} express the recombination effects and G_m for the effect of stimulated emission. R_{ph} and G_{ph} model the time-based change in photon density under spontaneous and stimulated emission effects that are determined by G_{k1} and G_{k2}, respectively. E_{out} produces the optical output power of the laser in the form of a voltage. Geometric parameters are specified in Table 1.

IV. Simulation Results

At first, we study of coverage factor effect on the L-I characteristic of QD laser. Fig. 3 shows L-I characteristic of QD lasers for different values of ξ=*0.07, 0.1, 0.2, 0.4,* when τ_{qr}=*0.5ns*, τ_r=*2.8ns* and τ_0=*10ps*.

As shown in the figure, the threshold current increases as the QD coverage factor increases more than 0.1, due to the increase in QD volume density, and as the result of need for more carriers in order to provide population inversion. On the other hand, the increase of coverage leads to a smaller *P* (occupation probability in the QD ground state), and this, in turn, leads to shorter relaxation time.

Consequently, there is an increase in quantum efficiency and output power. Numerical results reported in Fig. 4 shows the L-I characteristic for Γ_0, as the variable parameter Γ_0=5, 10, 20, 30, 40meV, when τ_{qr}=*0.5ns,* τ_r=*2.8ns* and τ_0=*10ps*. It is clear that the decrease in the line width $\boldsymbol{\Gamma_0}$ will have the same effect as coverage on the L-I curve of QD lasers. As it can be seen, the decrease of Γ_0 leads to the increase of the optical gain [see (1)], the result is a smaller *P* in the leasing, shorter relaxation lifetime and hence, the increase of quantum efficiency and laser output power.

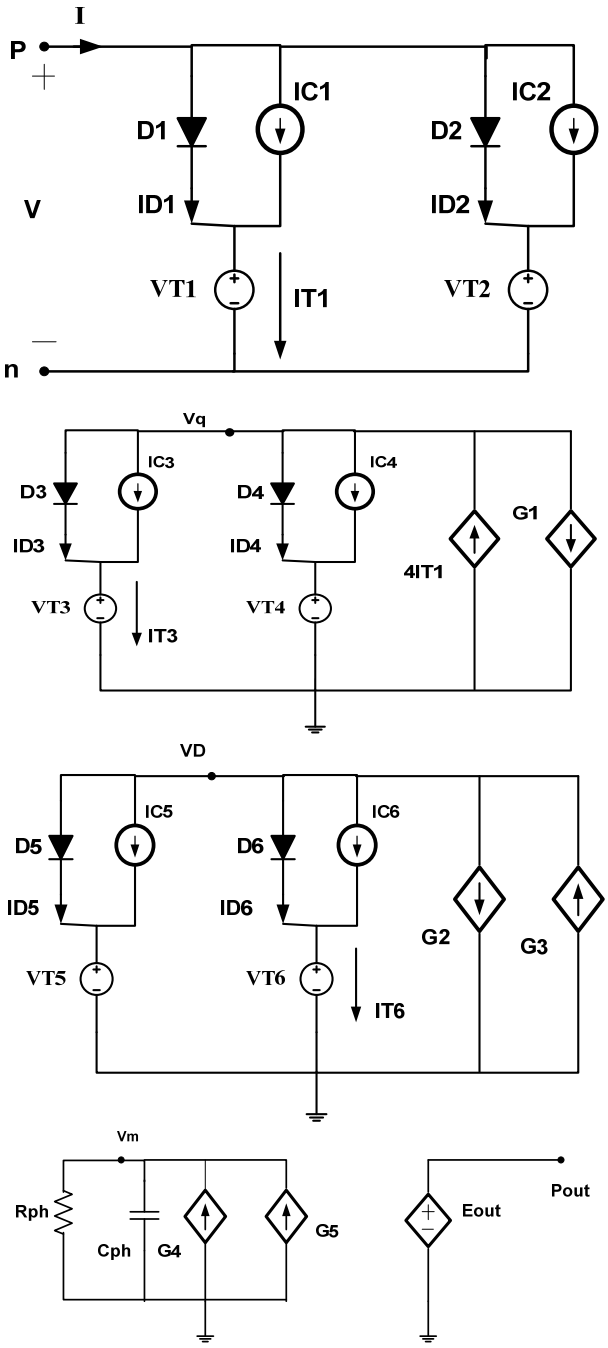

Fig. 2. An equivalent circuit mode for SA QD lasers

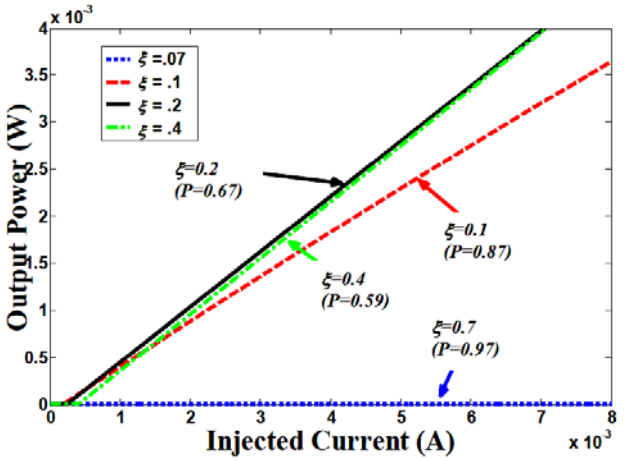

Fig. 3. Output power versus injected current with τ_{qr}=*0.5ns*, τ_r=*2.8ns* and τ_0=*10ps* and variable parameter of ξ=*0.07, 0.1, 0.2, 0.4*

TABLE I
TYPICAL PARAMETERS USED IN SIMULATION [2]

Symbol	Quantity	Value
ξ	Coverage factor of QDs	20%
τ_0	Carrier Relaxation Lifetime	10psec
Γ_0	Inhomogeneous Broadening	20meV
τ_s	Carrier Capture in SCH Region	1psec
η_c	Output Power Coupling Coefficient	0.449
τ_{sc}	Spontaneous Emission Lifetime in SCH	2.8nsec
V_a	Active Region Volume	$6.3\times10^{-16}m^3$
τ_e	Carrier Emission Time From QD to QW	0.2nsec
τ_{qr}	Carrier Recombination Lifetime in QW	1nsec
τ_r	Recombination Lifetime in QD	2.8nsec
τ_p	Photon Lifetime in the Cavity	8.8psec
ε_m	Phenomenological Gain-Saturation Term	$1.045\times10^{-22}m^3$
N_D	QD Volume Density	$9\times10^{-22}m^{-3}$
n_s, n_q n_D	SCH, QW and QD Diode Ideality Factors	2
R	Radius of a QD (Cylindrical Shape)	8nm
H	Height of a QD (Cylindrical Shape)	8nm
R_1	Right Facet Reflectivity	30%
R_2	Left Facet Reflectivity	90%
L	Cavity Length	900μm
Γ	Optical Confinement Factor	6%
α_i	Intrinsic Absorption Coefficient	$6cm^{-1}$
n_r	Refractive Index	3.5
β	Spontaneous Emission Coupling Efficiency	10^{-4}
Δ	Spin-Orbit Interaction Energy of QD Material	0.35eV
E_g	Band-gap	0.8eV

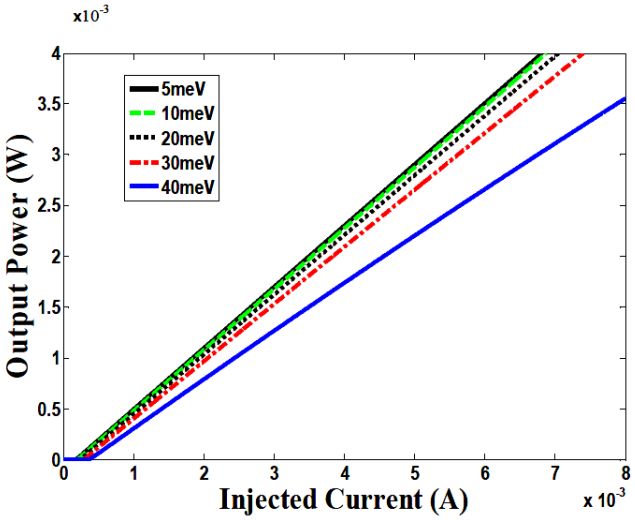

Fig. 4. Output power versus injected current with τ_{qr}=0.5ns, τ_r=2.8ns and τ_0=10ps and variable parameter of Γ_0=5, 10, 20, 30 and 40meV

Now, we will study the coverage effect over 3dB bandwidth. Fig. 5 shows the dependence of 3dB bandwidth, as a function of coverage factor with Γ_0=20meV and τ_{qr}=2.8ns, τ_r=2.8ns and τ_0=10ps.

As shown in Fig. 5, the increase in coverage factor due to the increase in the volumetric density of QDs (N_D) leads to the decrease in P, i.e. the occupation probability in the QD ground state. As the occupation probability in the QD ground state decreases, the relaxation rate increases for the carrier inside the QD, and this leads to the increase in 3dB bandwidth. As it can be observed from $f_{3dB}=(2\pi\tau_d)^{-1}$, the 3dB bandwidth is constrained by the time constant τ_d. Finally, Fig. 6 deals with the analysis of the simultaneous effect of the relaxation time constant and coverage factor over 3dB frequency.

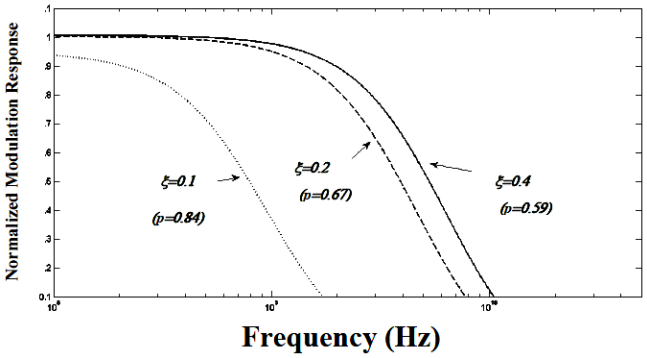

Fig. 5. Modulation response of QD laser for different coverage ξ=0.1, 0.2, 0.4 with Γ_0=20meV and τ_0=10psec, τ_{qr}=2.8nsec and τ_r=2.8nsec

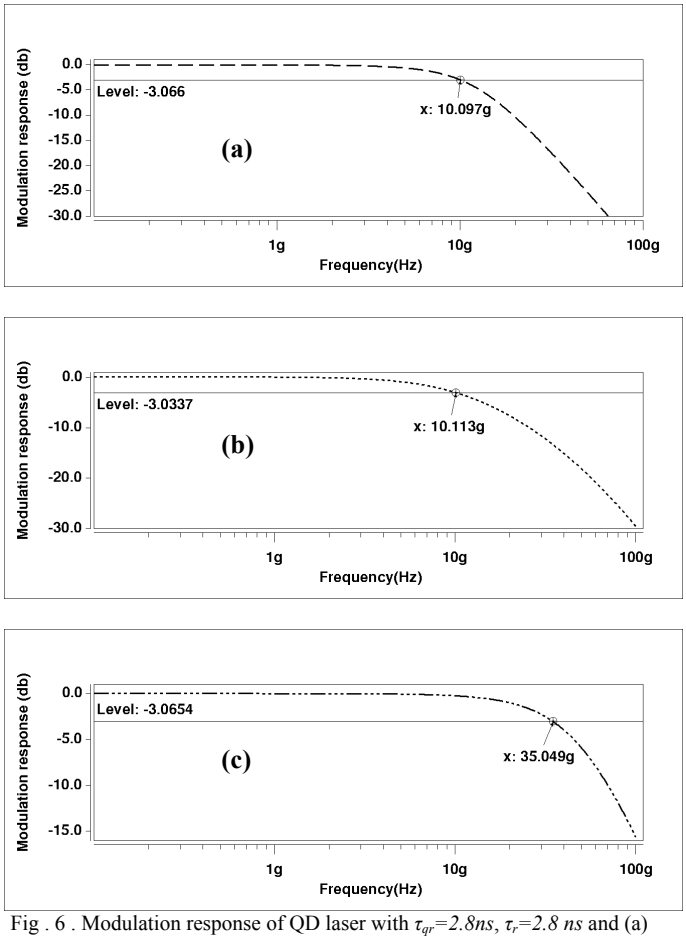

Fig . 6 . Modulation response of QD laser with τ_{qr}=2.8ns, τ_r=2.8 ns and (a) τ_0=3ps, ξ =0.1, (b) τ_0=7ps , ξ=0.4, (c) τ_0=1ps , ξ=0.4 , Γ_0 = 5meV.

As it can be observed in Fig. 6(a) and 6(b), we need τ_0=3ps ξ=0.1 and τ_0=7ps, ξ=0.4 for the signal modulation of 10GHz. Fig. 6(c) shows that for a 35GHz, we need τ_0=1ps, ξ=0.4 , Γ_0 = 5meV, the requirements for relaxation lifetime are much more severe in high-speed modulation relative to the static conditions [8].

The above results reveal that if the relaxation lifetime decreases to 1ps (and at the same time coverage factor increases to 0.4 and line width Γ_0 decreases to less than

ISBN: 978-988-19251-9-0
ISSN: 2078-0958 (Print); ISSN: 2078-0966 (Online)

10meV), then QD lasers, as high-speed modulation lasers, act with a chirp that is approximately equal to zero. Note that the *GHz* modulation of strained QW lasers is done by external QW modulators using quantum-confined stark effect. This is because, in strained QW lasers, wavelength chirp is an inevitable problem for high-speed modulation [8].

V. Conclusions

We used a reported circuit model for QD lasers based on standard rate equations to study the effects of some important parameters on the performance of these lasers. This circuit model is usefully able to explain the QD coverage factor behavior on threshold current, quantum efficiency, output power, and frequency response and 3dB bandwidth for QD lasers. Based on the simulation results, we realized that as the threshold current increases (as a result of increase in QD coverage factor) quantum efficiency and output power also increases. Besides, as the quantum-dot coverage factor increases, the occupation probability in the QD ground state decreases. This, in turn, decreases the relaxation lifetime for the carrier inside the QD, and as a result, the 3dB bandwidth increases. To achieve a high-speed modulation, higher than *10GHz*, not only the relaxation lifetime should be decreased to about 1ps, but also the QD coverage factor should also be increased and the line width should be decreased.

References

[1] M. Sugawara, N. Hatori, H. Ebe, and M. Ishida, "Modeling room-temperature lasing spectra of 1.3-μmself-assembled InAs/GaAs quantum-dot lasers: Homogeneous broadening of optical gain under current injection," J. Appl. Phys., vol. 97, no. 4, pp. 43 523–43 527, 2005.

[2] V. Ahmadi, and M. H. Yavari, "Circuit-Level Implementation of Semiconductor Self-Assembled Quantum Dot Laser," IEEE J.Sel. Topics in Quantum Electron. , vol. 15, no.3, pp. 774-779, May/June 2009.

[3] E. Mortazi, V. Ahmadi, and M. K. Moravvej-Farshi, "An integrated equivalent circuit model for relative intensity noise and frequency noise spectrum of a multimode semiconductor laser," IEEE J. Quantum Electron., vol. 38, no. 10, pp. 1366–1371, Oct. 2002.

[4] P. V. Mena, "Circuit-level modeling and simulation of semiconductor lasers," Ph.D. dissertation, Univ. Illinois, Chicago, 1998.

[5] M. F. Lu, J. S. Deng, C. Juang, M. J. Jou, and B. J. Lee, "Equivalent circuit model of quantum well lasers," IEEE J. Quantum Electron., vol. 31, no. 8, pp. 1418–1422, Aug. 1995.

[6] S. A. Javro and S. M. Kang, "Transforming Tucker's linearized laser rate equations to a form that has a single solution regime," J. Lightwave Technol., vol. 13, no. 9, pp. 1899–1904, Sep. 1995.

[7] P. V. Mena, S. M. Kang, and T. A. De Temple, "Rate-equation-based laser models with a single solution regime," J. Lightwave Technol., vol. 15, no. 4, pp. 717–730, Apr. 1997.

[8] M. Sugawara, *Self-assembled InGaAs/GaAs quantum dots in Semiconductors and Semimetals,* vol. 60, M. Sugawara, Ed. San Diego, CA: Academic, 1999.

[9] M. Sugawara, "Effect of carrier dynamics on quantum-dot laser performance and possibility of bi-exciton lasing," in Proc. SPIE, vol. 3283, pp. 88–99, 1998.

[10] A. Sakamoto and M. Sugawara, "Theoretical calculation of lasing spectra of quantum-dot lasers: Effect of homogeneous broadening of optical gain," IEEE Photon. Technol. Lett., vol. 12, no. 2, pp. 107–109, Feb. 2000.

[11] R. S. Tucker and D. J. Pope, "Circuit modeling of the effect of diffusion on damping in a narrow-stripe semiconductor laser," IEEE J. Quantum Electron., vol. QE-19, no. 7, pp. 1179–1183, Jul. 1983.

[12] J. Katz, S. Margalit, C. Harder, D. Wilt, and A. Yariv, "The intrinsic electrical equivalent circuit of a laser diode," IEEE J. Quantum Electron., vol. QE-17, no. 1, pp. 4–7, Jan. 1981.

ISBN: 978-988-19251-9-0
ISSN: 2078-0958 (Print); ISSN: 2078-0966 (Online)